A STUDY OF FORCED CONVECTION WITHIN A HORIZONTAL CAVITY WITH NINE NON-ROTATING HEATED CYLINDERS

Paulo Mohallem Guimarães
Universidade Federal de Itajubá – UNIFEI
Departamento de Engenharia Mecânica
Avenida BPS, 1303 – Pinheirinho – Itajubá – MG – 37500-176
paulomgui@uol.com.br

Rogério José da Silva
rogeriojs@unifei.edu.br

Genésio José Menon
genesio@unifei.edu.br

Abstract. In this work the forced convection is analyzed in a horizontal cavity with all walls being insulated and one cooled. There are 9 non-rotating heated cylinders inside the cavity. The flow is induced by one fan placed near the upper horizontal wall. No buoyancy forces are considered. The finite element method is applied to solve the continuity, momentum, and energy equations using 4-node elements. Furthermore, the Petrov-Galerkin method and the penalty technique are applied to deal with difficulties in the convective and pressure terms, respectively. Numerical and experimental comparisons are also carried out to validate the computational code. Temperature and velocity distributions are presented showing their correlation with the Nusselt number behavior for various Reynolds numbers.Some recirculations are found that work as isolations layers that make heat transfer more difficult.

Keywords: finite element method, cylinder, Petrov-Galerkin, convective heat transfer, laminar flow

1. Introduction

The study of natural, mixed, and forced convection in enclosures have been carried out for decades due to their importance in engineering applications such as solar energy systems, electronic cooling equipments, heat exchangers, etc.

In Fu et al. (1994), a penalty finite-element numerical method is used to investigate enhancement of natural convection of an enclosure by a rotating circular cylinder near a hot wall. They conclude that the direction of the rotating cylinder plays a role in enhancing natural convection in an enclosure. In this study, the counter-clockwise rotating cylinder apparently contributes to the heat transfer rate, but the clockwise rotating cylinder does not. When the value of the Richardson number is about 10^3, the enhancement of the heat transfer rate begins to be revealed. The maximum enhancement of the heat transfer is approximately equal to 60%.

Nguyen et al. (1996) investigate numerically the heat transfer from a rotating circular cylinder immersed in a spatially uniform, time-dependent convective environment including the effects due to buoyancy force. The flow equations, based on the vorticity and stream function, are solved along with the energy equation by a hybrid spectral scheme that combines the Fourier spectral method in the angular direction and a spectral element method in the radial direction. Several cases are simulated for Grashof numbers up to 2×10^4, Reynolds numbers up to 200, and a range of speed of rotation from –0.5 to +0.5. The results show that vortex shedding is promoted by the cylinder rotation but it is vanished by the presence of the buoyancy force. In opposing flows, the counter flow currents cause a large expansion of the streamlines and isotherms in the direction normal to the free stream velocity. These changes in the structure of the flow and the temperature fields greatly modify the heat flux along the surface of the cylinder and consequently, the heat transfer rate is strongly dependent upon Reynolds number, Grashof number, rotational speed, and the gravity direction. Effects due to pulsation are also reflected in the Nusselt number history in the form of periodic oscillations.

Lee et al. make experimental investigations to study the convective phenomena of an initially stratified salt-water solution due to bottom heating in a uniformly rotating cylindrical cavity. Three types of global flow patterns initially appear depending on the effective Rayleigh number and Taylor number: stagnant flow regime, single mixed layer flow regime and multiple mixed layer flow regime. The number of layers at its initial stage and the growth height of the mixed layer decreases for the same Rayleigh number. It is ascertained in the rotating case that the fluctuation of interface between layers is weakened, the growth rate of mixed layer is retarded and the shape of interface is more regular compared to the stationary case.

Joo-Sik Yoo (1998) studies numerically the mixed convection in a horizontal concentric annulus with Prandtl number equal to 0.7. The inner cylinder is hotter than the outer cylinder. The forced flow is induced by the cold outer cylinder that rotates slowly with constant angular velocity with its axis at he center of the annulus. Investigations are made for various combinations of Rayleigh number Ra, Reynolds number Re, and ratio σ of the inner cylinder diameter

to the gap width, that is, Ra $\leq$ 5 x 10^4, Re $\leq$ 1500, and 0.5 $\leq$ σ $\leq$ 5. The flow patterns can be categorized into three types according to the number of eddies: two-one- and no-eddy flows. The transitional Reynolds number between two-and one-eddy flows for small Rayleigh number is not greatly affected by the geometrical parameter σ. Net circulation of fluid in the direction of cylinder's rotation is decreased as Ra is increased. As the speed of the cylinder's rotation is increased, the points of maximum and minimum local heat fluxes at both of the inner and outer cylinders move in the same direction of cylinder's rotation for small Ra, but for high Ra the points at the inner cylinder do not always move in the same direction. Overall heat transfer at the wall is rapidly decreased, as Re approaches the transitional Re between two- and one-eddy flows.

Lin and Yan (2000) conducted an experimental study through temperature measurements to investigate the thermal features induced by the interaction between the thermal buoyancy and rotation-induced Coriolis force and centrifugal force in an air-filled heated inclined cylinder rotating about its axis. Results are obtained ranging the thermal Rayleigh number, the Taylor number, the rotational Rayleigh number, and the inclined angle. The experimental data suggest that when the cylinder is stationary, the thermal buoyancy driven flow is random oscillation at small amplitude after initial transient for inclined angle smaller than 60°. Rotating the cylinder is found to destabilize the temperature field when the rotation speed is less than 30 rpm and to stabilize it when the rotation speed exceeds 30 rpm. Moreover, the distributions of time-average temperature in the Z-direction for various inclined angles become widely separate only at low rotation rates less than 60 rpm.

In this work, a forced convection study in a rectangular cavity with a set o nine non-rotating heated cylinders on the upper right corner is carried. This particular problem can be applied to the study of heat exchangers in industrial ovens. This dimensionless study holds a laminar and unsteady regime whereas some results are shown for the steady regime.

2. Geometry and boundary conditions

Figure 1 shows the geometry and the mesh used, while the boundary conditions are as follows:

On S_1: $U = V = 0$ and $\dfrac{\partial \theta}{\partial X} = 0$ or $\dfrac{\partial \theta}{\partial Y} = 0$;

On S_2: $U = V = 0$ and $\theta = 0$; $\qquad\qquad\qquad\qquad\qquad\qquad\qquad\qquad$ (1)

On S_3: $U = V = 0$ and $\theta = 1$;

On S_4: $U = 1$ and $V = 0$;

where U and V are the dimensionless velocity components on X and Y directions, respectively, while θ is the dimensionless temperature.
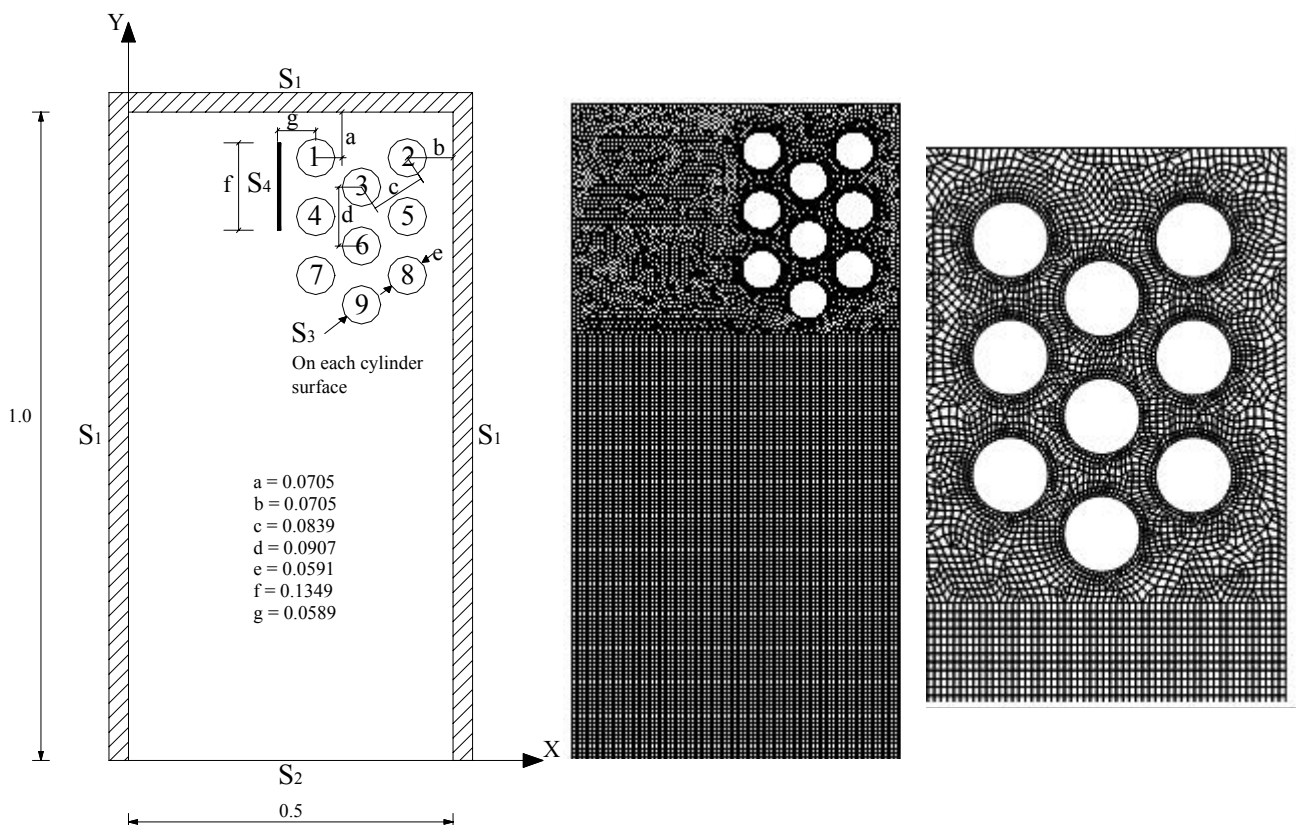
Figure 1. Geometry and mesh with 16448 structured and non-structured elements.

3. Problem formulation

The problem governing equations are given by the equations of mass conservation, Navier-Stokes, and energy. Being that u and v are the velocity components, T is the fluid temperature, t' is the time field, D_T is the thermal diffusivity, β_T is the thermal expansion coefficient, ν is the kinematic viscosity, g is the gravitational acceleration, ρ_0 is the fluid density and T_0 is the reference temperature taken as $T_0 = T_c$.

Under the Boussinesq approximation and the following dimensionless parameters:

Under the Boussinesq approximation and the following dimensionless parameters:

$$X = \frac{x}{H}; \quad Y = \frac{y}{H}; \quad U = \frac{u}{U_0}; \quad V = \frac{v}{U_0}; \quad P = \frac{p}{\rho_0 U_0^2}; \quad \tau = \frac{t}{(H/U_0)}; \quad \theta = (T - T_0)/\Delta T; \quad \Delta T = T_h - T_c; \tag{2}$$

$$Pr = \frac{\nu}{D_T}; \quad Re = \frac{U_0 \rho_0 H}{\mu};$$

which are named as the Prandtl number Pr, the Reynolds number Re, the reference velocity U_0, and the dynamic viscosity μ, the dimensionless governing equations can be cast into the following form:

$$\frac{\partial U}{\partial X} + \frac{\partial V}{\partial Y} = 0; \tag{3}$$

$$\frac{\partial U}{\partial \tau} + U\frac{\partial U}{\partial X} + V\frac{\partial U}{\partial Y} = -\frac{\partial P}{\partial X} + \frac{1}{Re}\left(\frac{\partial^2 U}{\partial X^2} + \frac{\partial^2 U}{\partial Y^2}\right); \tag{4}$$

$$\frac{\partial V}{\partial \tau} + U\frac{\partial V}{\partial X} + V\frac{\partial V}{\partial Y} = -\frac{\partial P}{\partial Y} + \frac{1}{Re}\left(\frac{\partial^2 V}{\partial X^2} + \frac{\partial^2 V}{\partial Y^2}\right); \tag{5}$$

$$\frac{\partial \theta}{\partial \tau} + U\frac{\partial \theta}{\partial X} + V\frac{\partial \theta}{\partial Y} = \frac{1}{Re\,Pr}\left(\frac{\partial^2 \theta}{\partial X^2} + \frac{\partial^2 \theta}{\partial Y^2}\right). \tag{6}$$

The average Nusselt number along a surface S can be written as:

$$Nu = \frac{1}{S}\int_S \frac{\partial \theta}{\partial n}\, ds. \tag{7}$$

where n means the direction perpendicular to the surface S which can be the hot, cold, or cylinder surface.

4. The solution method

By applying the Petrov-Galerkin formulation to the equations above, Eqs. (3) to (6), together with the Penalty technique , the weak form of the conservation equations is as follows:

$$\int_\Omega N_i\left[\frac{\partial U}{\partial t} + \frac{1}{Re}\left(\frac{\partial N_i}{\partial X}\frac{\partial U}{\partial X} + \frac{\partial N_i}{\partial Y}\frac{\partial U}{\partial Y}\right)\right]d\Omega + \int_\Omega^R \lambda\frac{\partial N_i}{\partial X}\left(\frac{\partial U}{\partial X} + \frac{\partial V}{\partial Y}\right)d\Omega =$$
$$\int_\Omega (N_i + P_{il})\left(U\frac{\partial U}{\partial X} + V\frac{\partial U}{\partial Y}\right)d\Omega - \int_{\Gamma_0} N_i\, p\, n_x\, d\Gamma \quad ; \tag{8}$$

$$\int_\Omega N_i \left[\frac{\partial V}{\partial t} + \frac{1}{Re} \left(\frac{\partial N_i}{\partial X} \frac{\partial V}{\partial X} + \frac{\partial N_i}{\partial Y} \frac{\partial V}{\partial Y} \right) \right] d\Omega + \int_\Omega^R \lambda \frac{\partial N_i}{\partial Y} \left(\frac{\partial U}{\partial X} + \frac{\partial V}{\partial Y} \right) d\Omega =$$

$$\int_\Omega \left[(N_i + P_{i1}) \left(U \frac{\partial V}{\partial X} + v \frac{\partial V}{\partial Y} \right) \right] d\Omega - \int_{\Gamma_0} N_i p\, n_y \, d\Gamma \tag{9}$$

$$\int_\Omega \left[N_i \frac{\partial \theta}{\partial t} + \frac{1}{Re\,Pr} \left(\frac{\partial N_i}{\partial x} \frac{\partial \theta}{\partial x} + \frac{\partial N_i}{\partial y} \frac{\partial \theta}{\partial y} \right) \right] d\Omega = \int_\Omega (N_i + P_{i2}) \left(u \frac{\partial \theta}{\partial x} + v \frac{\partial \theta}{\partial y} \right) d\Omega + \int_{\Gamma_1} N_i q \, d\Gamma \, ; \tag{10}$$

where q = 0 (no heat flux). The dependent variables are approximated by:

$$\Phi(X,Y,t) = \sum_j N_j(X,Y)\Phi_j(t) \; ; \; p(X,Y,t) = \sum_k M_k(X,Y)p_k(t). \tag{11}$$

N_i and N_j denote the linear shape functions for Φ, that is, for U, V, and θ, and M_k denote the shape functions for the constant piecewise pressure. P_{ij} are the Petrov-Galerkin perturbations applied to the convective terms only. The terms P_{ij} are defined as follows:

$$P_{ij} = k_j \left(U \frac{\partial N_i}{\partial X} + V \frac{\partial N_i}{\partial Y} \right); \; k_j = \frac{\alpha_j \overline{h}}{|V|}; \; \alpha_j = \coth \frac{\gamma_j}{2} - \frac{2}{\gamma_j} \; ; \; \gamma_j = \frac{|V|\overline{h}}{\varepsilon_j} \; ; \; j = 1,2 \tag{12}$$

where γ is the element Péclet number, $|V|$ is the absolute value of the velocity vector that represents the fluid average velocity within each element, $\overline{h}$ is the element average size, $\varepsilon_1 = 1/Re, \varepsilon_2 = 1/Pe$, and λ is the Penalty parameter which is considered to be 10^9. The time integration is by a semi-implicit backward Euler method. Moreover, the convective terms are calculated explicitly and the viscous and Penalty terms implicitly. The temperatures and velocities are interpolated by using the four-node quadrilateral elements and the pressure by the one-node ones. Finally, the reduced integration is applied to the penalty term to avoid numerical locking.

The algorithm is extensively validated by comparing the results of the present work with both the ones obtained in experimental and numerical investigations. The first comparison is accomplished not only by using the experimental results presented by Lee and Mateescu (1998) and Armaly (1983) et al., but also by the numerical ones achieved by Lee and Mateescu (1998), Gartling (1990), Kim and Moin (1985), and Sohn (1988). The air flow of the present comparison analysis is taken as bidimensional, laminar, incompressible, and under the unsteady regime. The domain is a horizontal upstream backward-facing step channel whose inlet has a fully developed velocity profile given by $u = 24y(0.5-y)\overline{U}$ and $v = 0$ in which Re = 800.

Table (1) shows the results from the first comparison for the flow separation distance Xs on the upper surface and its reattachment distance Xrs. As for the bottom surface, the comparison is made on the reattachment distance Xr. As it can be noticed, the results of the present work agree well with the ones from the literature.

Table1. Comparison of computed predictions and experimental measurements of dimensionless lengths (with respect to the channel height) of separation and reattachment on upper and lower walls.

		Experimental results			Computed results			
	Length on	Lee and Mateescu (1998)	Armaly et al. (1983)	Present prediction	Gartling´s prediction (1990)	Kim & Moin (1985)	Lee and Mateescu (1998)	Sohn (1988)
Lower Wall	x_r	6.45	7.0	5.75	6.1	6.0	6.0	5.8
Upper Wall	x_s	5.15	5.7	4.95	4.85	-	4.8	-
	x_{rs}	10.25	10.0	9.9	10.48	-	10.3	-
	$x_{rs}-x_s$	5.1	4.3	4.95	5.63	5.75	5.5	4.63
Reynolds		805	800	800	800	800	800	800
Hd/Hu		2	1.94	2	2	2	2	2

The second comparison is performed with the numerical results shown by Comini (1997) et al.. The contrasting study is carried out by considering a problem involving a Poiseiulle flow heated from below with velocity and temperature profiles at the inlet given by U =6Y(1-Y) and θ = 1-Y, respectively. The flow is considered to be

bidimensional, laminar, and incompressible in the unsteady regime. In this case, some values are chosen such as Re=10, Pr = 0.67, and Fr = 1/150. The grid has 4000 quadrilateral four-noded elements with $\Delta x = 0.1$, $\Delta y = 0.15$, $\Delta t = 0.01$ and 1000 iterations. After approximately iteration 500, the regime turns to be quasi-periodic with the average Nusselt number on the upper wall oscillating around a mean value of 2.44. This value agrees satisfactorily with the one found by Comini (1997) et al. which is 2.34, resulting in a deviation of about 4%.
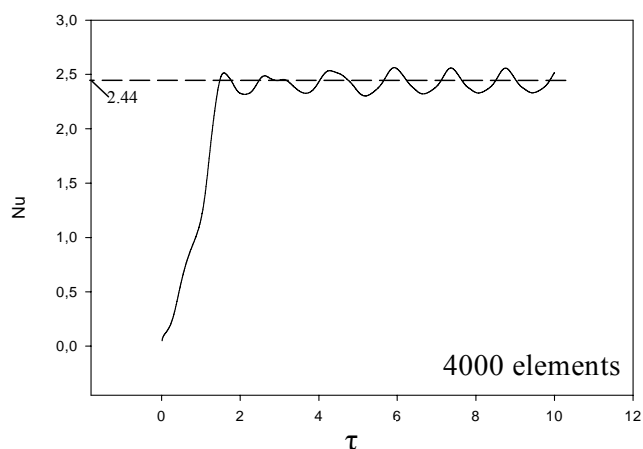
Figure 2. Average Nusselt number Nu measured along the upper surface versus time for a Poiseuille flow heated from below.

The third case studied to validate the mathematical modeling code is featured by mixed convection of air between two horizontal concentric cylinders with a cooled rotating outer cylinder with Pr = 0.7, Re = 10, 50, 100, 150, 200, 250, 300, 350, and 500, and Ra = 10^4, 2 x 10^4, and 5 x 10^4. The domain is discretized spatially with 5976 non-structured four-node quadrilateral elements.

Figure 3 shows the average Nusselt numbers (inner cylinder and outer cylinder surfaces) from the present work compared to the ones found in Yoo (1998), where different grids are used: meshes of (65X64), (45 x 64), or (65 x 32) for a finite difference scheme. In fact, the results found here are higher than the ones in Yoo(1998). This difference is likely due to different methods and different meshes. The time step used is 0.01 for almost all cases and the number of iterations ranges from 10^4 to $3x10^4$.
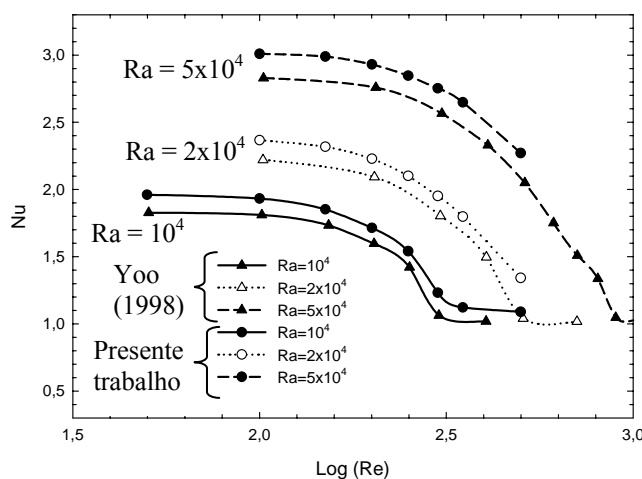
Figure 3. Average Nusselt number versus Reynolds number for the third comparison.

5. Results

Figure 4 shows temperature, velocity, and streamline distributions for Reynolds number Re = 100, 250, 750, and 1000. The streamlines are only shown to assure the understanding of flow directions and recirculations. The velocity intensity can be seen through the velocity vector behaviour. For all cases, there are two opposite recirculations before the flow entrance between cylinders 1 and 4. Although the size of these two recirculations tend to decrease as Re increases, more intense velocities are present for Re = 1000. All flows are mainly governed by two big cells. Interestingly, for high Re, the cells near the cold surface do not get smaller as Re increases. The other cell velocities get much stronger as Re increases. As for the temperature, the cold fluid tends to be confined near the cold wall. However, for Re = 1000, this cold fluid tries to fin its way along the right insulated wall.
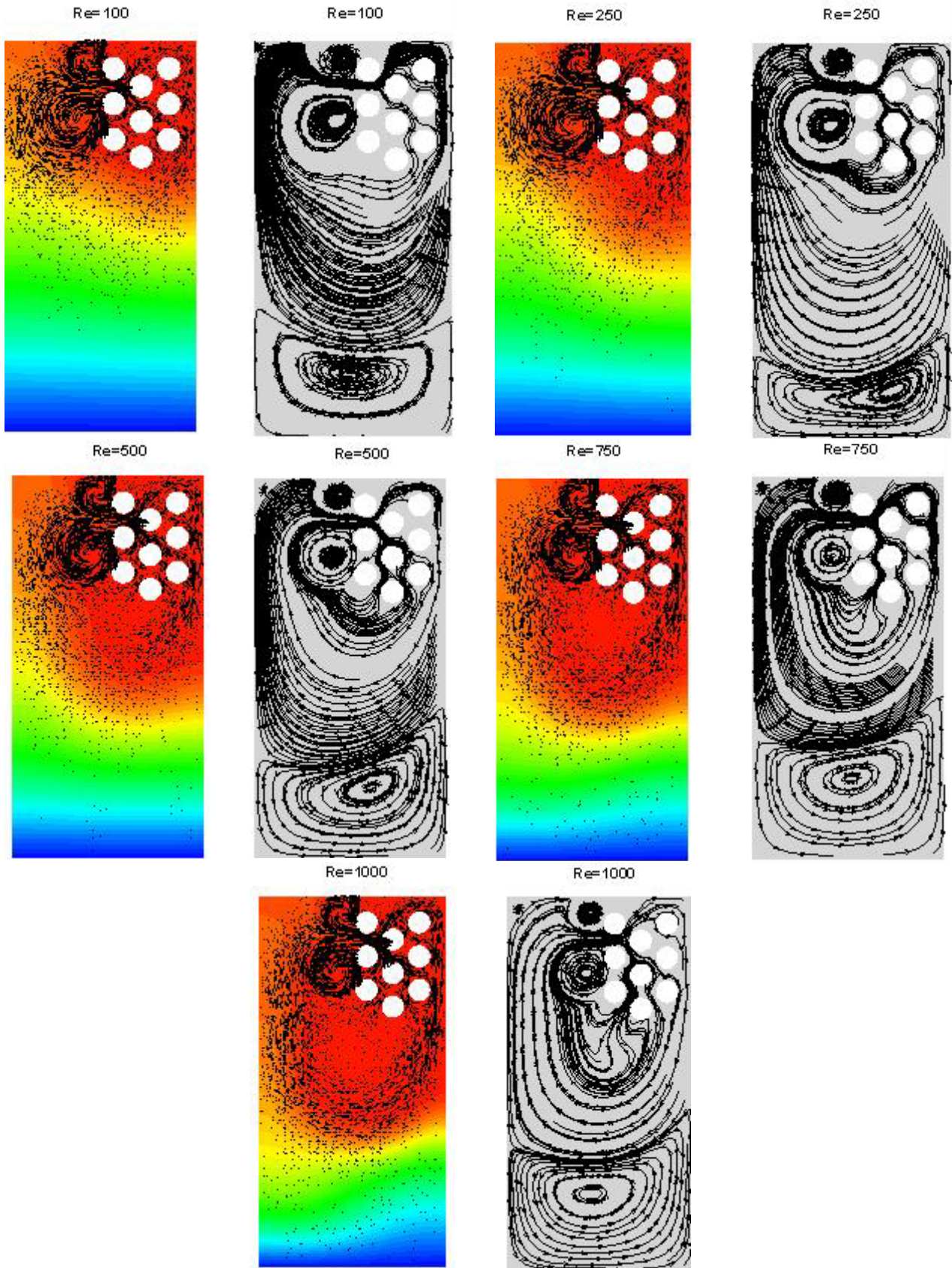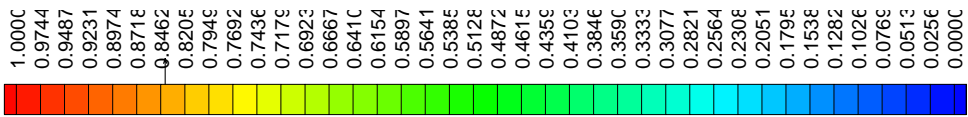
Figure 4 – Isotherms, velocity vectors, and streamlines for Re = 100, 250, 500, 750, and 1000.

Since flows through the cylinders are quite complex, Fig. 5 pictures them in more detailed views for Re = 100, 250, 500 and 1000.The recirculations in front of cylinders 1, 4, and 7 are due to the presence of stronger pressure gradients caused by flows through the cylinders originated from a main flow between cylinders 1 and 4. From this main flow, three strong ones are branched out after reaching cylinder 3. Two of them are then responsible for blocking some passages and, hence, creating those two main recirculations in front of cylinders 1, 4, and 7. One can observe that the flow is almost stagnant between cylinders 3 and 5, and 6 and 9. This may not contribute to heat transfer. The flow on the right hand side of cylinders 2, 5, and 8 is almost one-dimensional. As Re increases, the temperature distribution tends to be uniform. It seems that as Re increases, a recirculation starts after cylinder 9.
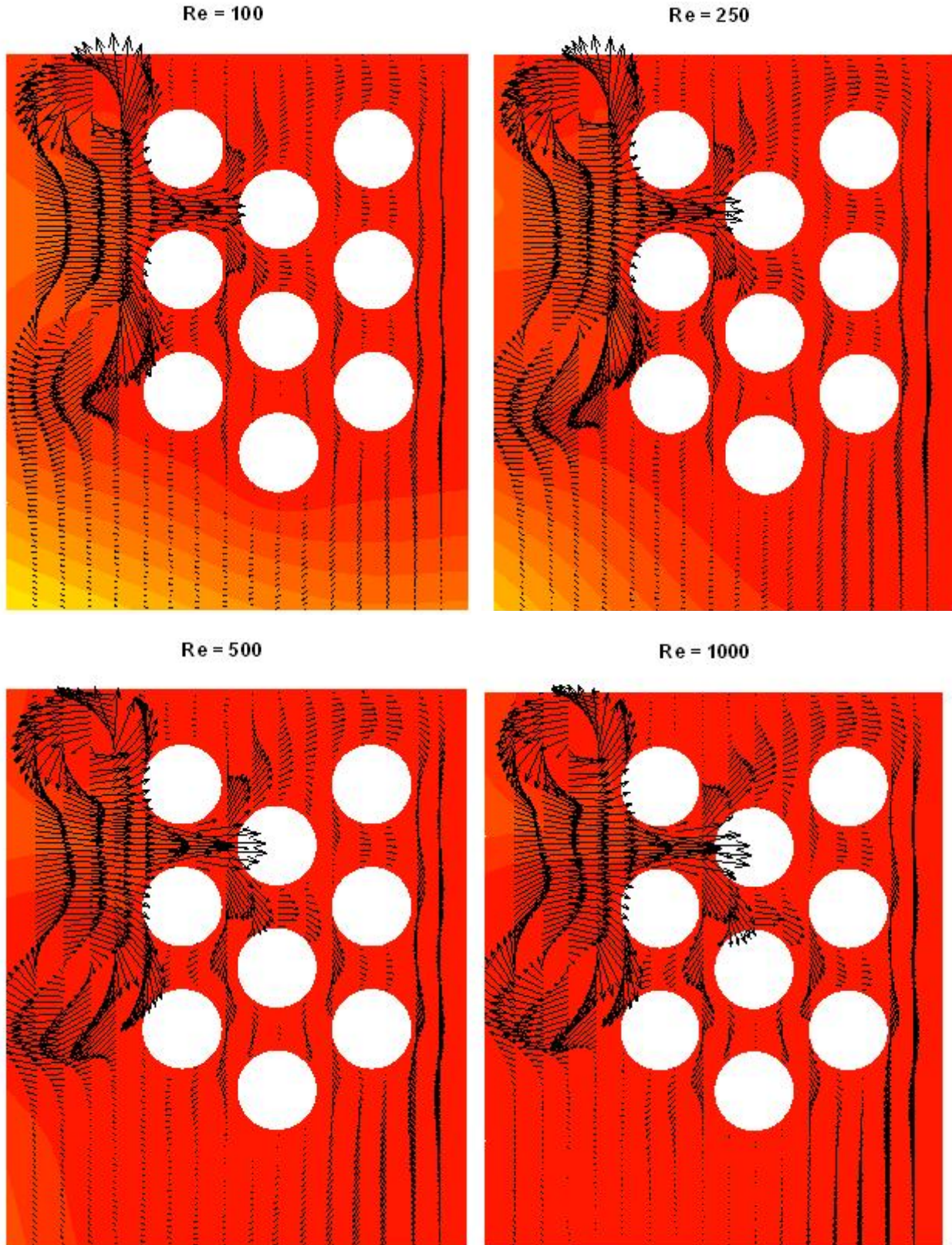
Figure 5 – Detailed view of the velocity vectors around the cylinders.

Figure 6 shows the Nusselt number behaviour in time for Re = 100, 250, 500, and 1000. The Nusselt numbers are calculated on the cold wall NUc, on all cylinder surfaces together NUcyl, and on each cylinder surface NUcyl(i), where i = 1, 2,….., 9. Cylinders 1, 3, and 4 have the highest NU through time. It is worth observing that NUcyl(1)is smaller than NUcyl(4) for Re = 100 and 250. For higher Re, this behaviour is just the opposite. This can be explained by the ascendant flow of hot fluid around cylinder 7 which is higher as Re increases. The temperature distribution also features this behaviour due to its weaker uniformity around cylinder 1. Flow tends to be stronger through cylinders 1 and 3, and 2 and the insulated walls for higher Re.
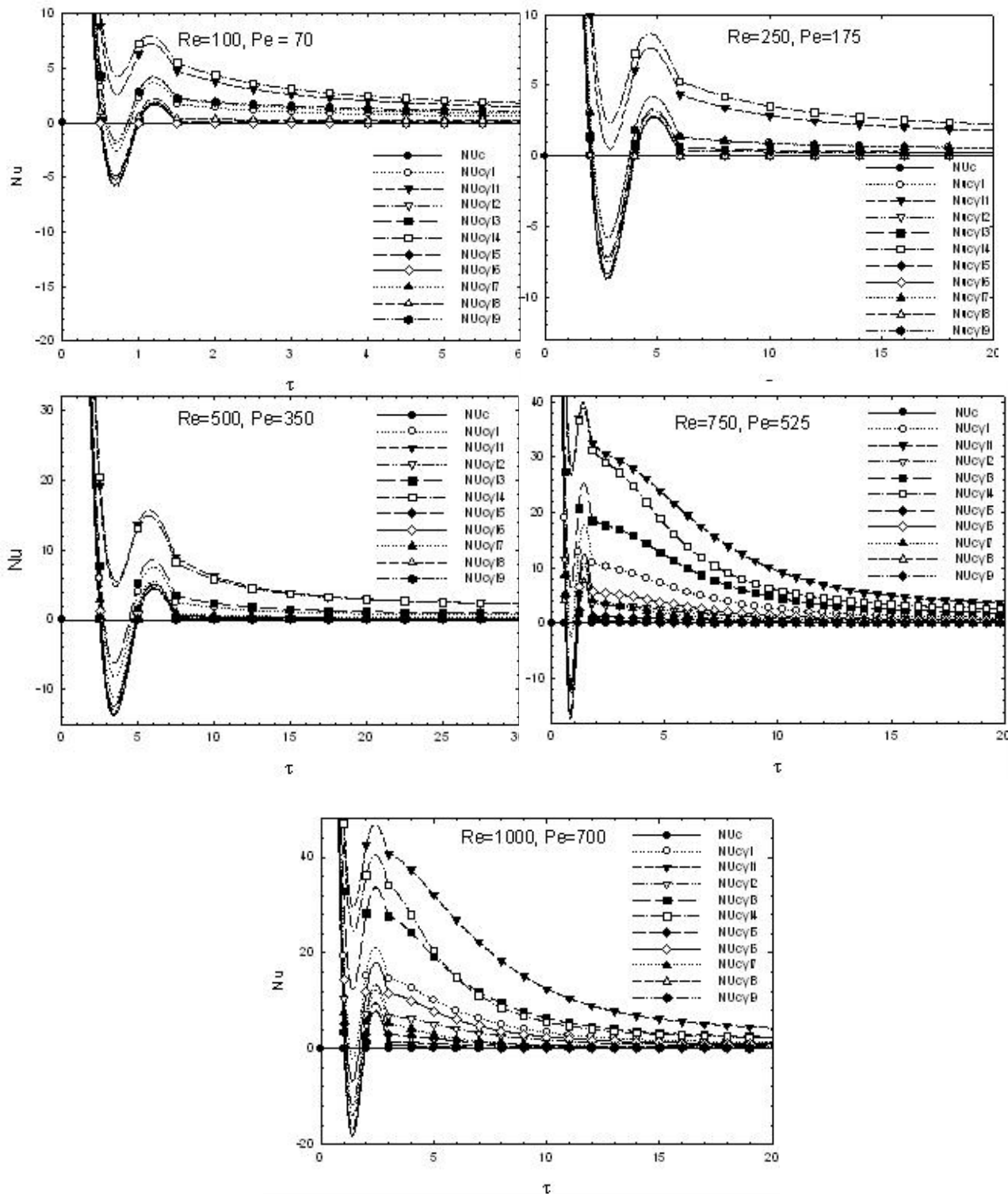
Figure 6 – Average Nusselt number versus time for Re = 100, 250, 500, 750, and 1000.

Finally, Fig. 7 presents the average Nusselt number in the steady state regime for Re = 100, 250, 500, 750, and 1000. Again, the higher Re is, the higher NUcyl(1) gets. However, for Re smaller than 500, NUcyl(4) is higher than NUcyl(1). It is interesting to notice how NUcyl(9) decreases and how NUcyl(3) increases. Furthermore, it can be noticed that NUcyl(2,5,7,8, and 9) are too small, and thus, featuring a weak heat transfer on those surfaces. Maybe, a way of enhancing it on those areas is to make wider passages in some places guaranteeing more cold fluid reaching those cylinders. The fact that those main recirculations appear near the cold wall is certainly an issue which should be worked on to enhance heat transfer. These recirculations work as isolation layers which inhibits hot fluid coming from the cylinders to reach directly the cold wall. If this is done, maybe the temperature distribution would be uniform. If some conductive bodies are placed within the cavity, certainly new recirculations would be brought up and therefore, again, the location of those recirculations would be extremely important in the uniformity of the temperature field. Although this is a start study, it gives important results on recirculations and their influence on heat transfer. This can provide time and money savings when trying to build such devices in food industry. More studies with higher velocities are encouraged by the authors for future works.
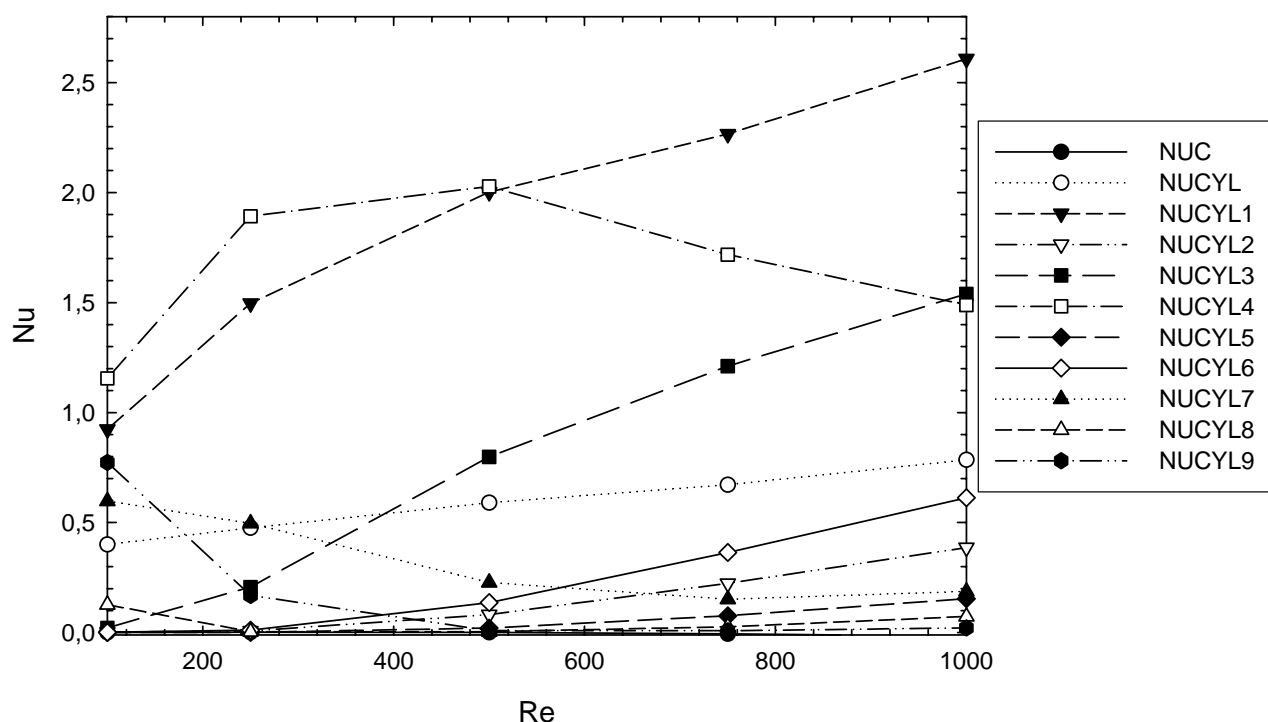
Figure 7 – Average Nusselt number for Re = 100, 250, 500, 750, and 1000.

6. Conclusions

In this work, the forced convection in a cavity with three isolated walls and one cooled wall is performed featuring a start study of heat exchangers in the food field. The governing equations are numerically solved using the finite element method with the Penalty technique on the convective terms. The method makes use of linear quadrilateral elements. Some comparisons are carried out to validate the computational code developed by the authors. Flow and temperature distributions are presented and some important results are reached by varying Reynolds number from 100 to 1000. There are some recirculations inside the cavity that are strongly correlated to the heat transfer and uniformity of temperature distribution. For all cases, a recirculation appears near the cold wall that works as an isolation layer and thus impairing heat transfer. The authors encourage some more studies in which the cylinders set configuration must be taken into account as well as higher forced velocities. Experimental studies have already been carried out by engineers from PRÁTICA TECHNOCOOK in the city of Pouso Alegre, Minas Gerais, Brazil.

7. Acknowledgements

8. References

Armaly, B. F., Durst, F., Pereira, and J. C. F. & Schonung, B., 1983, "Experimental and Theoretical Investigation of Backward-Facing Step Flow", Journal of Fluid Mechanics, Vol. 127, pp. 473-496.

Comini, G., Manzam, M. and Cortella, G., 1997, "Open Boundary Conditions for the Streamfunction-Vorticity Formulation of Unsteady Laminar Convection", Numerical Heat Transfer, Part B, Vol. 31, pp. 217-234.

Fu, W.S., Cheng, C.S. and Shieh, W.J., 1994, "Enhancement of Natural Convection Heat Transfer of an Enclosure by a Rotating Circular Cylinder", Int. J. Heat Mass Transfer, Vol. 37, No. 13, pp. 1885-1897.

Gartling, D. K., 1990, "A Test Problem for Outflow Boundary Conditions – Flow over a Backward-Facing Step", International Journal of Numerical Methods in Fluids, Vol. 11, pp. 953-967.

Kim, J. and Moin, P., 1985, "Application of a Fractional-Step Method to Incompressible Navier-Stokes Equations", Journal of Computational Physics, Vol. 59, pp. 308-323.

Lee, J., Kang, S. H. and Son, Y. S., 1999, "Experimental Study of Double-Diffusive Convection in a Rotating Annulus with Lateral Heating", Int. J. Heat Mass Transfer, Vol. 42, pp. 821-832.

Lee, T. and Mateescu, D., 1998, "Experimental and Numerical Investigation of 2-D Backward-Facing Step Flow", Journal of Fluids and Structures, Vol. 8, pp. 1469-1490.

Lin, D. and Yan, W.M., 2000, "Experimental Study of Unsteady Thermal Convection in Heated Rotating Inclined Cylinders", Int. J. Heat Mass Transfer, Vol. 43, pp. 3359-3370.

Nguyen, H. D., Paik, S. and Douglass, R. W., 1996, "Unsteady Mixed Convection About a Rotating Circular Cylinder with Small Fluctuations in the Free-Stream Velocity", Int. J. Heat Mass Transfer, Vol. 39, No. 3, pp. 511-525.

Sohn, J., 1998, "Evaluation of FIDAP on Some Classical Laminar and Turbulent Benchmarks", International Journal of Numerical Methods in Fluids, Vol. 8, pp. 1469-1490.

Yoo, J., 1998, "Mixed Convection of Air Between Two Horizontal Concentric Cylinders with a Cooled Rotating Outer Cylinder", Int. J. Heat Mass Transfer, Vol.41, No. 2, pp. 293-302.

9. Copyright Notice